Int. J. Nanosci. Nanotechnol., Vol. 8, No. 2, June 2012, pp. 111-120

Optical, Thermal and Structural Properties of CdS Quantum Dots Synthesized by A Simple Chemical Route

N. Qutub, S. Sabir*

Department of Chemistry, Aligarh Muslim University, Aligarh, 202002, India

(*) Corresponding author: sabirsuhail09@gmail.com
(Received:15 Jan. 2012 and Accepted: 25 Mar. 2012)

Abstract:
The present work deals with the synthesis and characterization of CdS nanoparticles with good thermal stability and optical properties by a novel and simple synthetic route. The nanoparticles were synthesized via chemical precipitation method in a single reaction vessel under ambient conditions. The prepared CdS nanoparticles were compared with the bulk CdS. The Optical properties were determined by using UV-Vis spectroscopy. The band gap from Absorption Spectra was found to be 2.66eV (470nm) while that of bulk is 2.42eV (515nm). Thermal properties were determined by DTA, TGA and DTG. The particles show good thermal stability with high melting point (~12500C). Structural and Morphological properties were analyzed by FTIR, XRD, SEM and TEM. The XRD pattern exhibit features of cubic crystal structure having morphology of octahedron and tetragonal phases. The particle size calculated from UV-Vis Spectroscopy, XRD and TEM was well below 10 nm.
Keywords: *Optical Properties, II–VI semiconductor CdS, Quantum dots, Quantum size effect, XRD.*

1. INTRODUCTION

Quantum dots are semiconductors whose electronic characteristics are closely related to the size and shape of the individual crystal. Generally, the smaller the size of the crystal, the larger will be the band gap, and greater will be the difference in energy between the highest valence band and the lowest conduction band. Therefore more energy is needed to excite the dot, and concurrently, more energy is released when the crystal returns to its resting state.

Due to quantum size effect, as the radius of the crystallite approaches the Bohr radius of an exciton, the energy gap begins to widen, quantization of the energy bands becomes apparent and a blue shift in the exciton transition energy can be observed [1-4]. The effective mass model is commonly used to study the size dependence of optical properties of Quantum Dots system [5]. CdS is insoluble in water, but soluble in dilute mineral acids. CdS shows variation in 1D morphology when the reaction conditions change (i.e. monomer concentration, reaction temperature and reaction time).

Any combination of reaction conditions could lead to diverse shapes such as dots, rods, bipods, tripods, tetrapods and spindles [6, 7]. CdS in bulk has hexagonal wurtzite -type structure with melting point 1600 ^{0}C [8]. CdS is an II –VI semiconductor consisting of cadmium from group II and sulfur from group VI of the periodic table of elements. Due to the cadmium surplus it exhibits intrinsic n-type of conductivity caused by sulfur vacancies and the depth of the acceptor level.

CdS bulk has band gap E_g=2.42 eV (515nm) [9] at room temperature and pressure. Nanostructured CdS have unique physical, chemical, electrical, optical and transport properties, which differ from the bulk material and even single atom. As the semiconductor nanoparticles exhibit size dependent

properties, the melting point of 2.5 nm CdS crystallites is as low as ~ 400^{0}C [8], the band gap of 0.7 nm CdS crystallites is 3.85 eV [10] and at very high pressure phase changes from hexagonal wurtzite type to rock salt cubic phase [11]. Since CdS has 2.42 eV (515 nm) band gap, so it is most promising candidate among II-VI compounds for detecting visible radiation [12].

As CdS nanoparticles (quantum dots) has wide band gap, it is widely used in optoelectronics, photonics, photovoltaics and photocatalysis. It is used as window material for hetero junction solar cells to avoid the recombination of photogenerated carriers which consequently improves the solar cells efficiency [13]. In optoelectronics, it is utilized for making photocells, light emitting diode (LED) [14, 15], lasers [16], and address decoders [17]. In photonics, CdS is employed to make nanocrystals [18], sensors [19], optical filters, and all optical switches [20]. In photovoltaics, it has been exploited to fabricate cadmium telluride (CdTe), as well as copper indium diselenide solar cells to act as a window layer that separates charge carriers produced due to photon absorption and photo detectors [21] and in the fabrication of thin film solar cells [20,22]. In photocatalysis, it is used for hydrogen production [23] and water purification [24]. CdS is also used as a pigment in paints and in engineered plastic for good thermal stability [25]. These properties are the result of high surface-to-volume ratio present in CdS nanoparticles.

In the present work, CdS nanoparticles were synthesized by single pot chemical precipitation method in aqueous medium using ambient reaction conditions. The Optical properties were determined by using UV-Vis spectroscopy, Thermal properties were determined by Thermal Gravimetric Analysis (TGA), Differential Thermogravimetry (DTG) and Differential Thermal Analysis (DTA), Structural and Morphological properties were analyzed by Fourier Transform Infrared Spectroscopy (FTIR) Spectroscopy, X-Ray Diffraction (XRD), Scanning Electron Microscopy (SEM) and Transmission Electron Microscopy (TEM). The particle size lied below 10 nm. The band gap lied at 2.66eV (470 nm). The XRD pattern exhibited features of cubic phase with octahedron and tetragonal morphologies. The particles showed good thermal stability.

2. MATERIAL AND METHODS

CdS nanoparticles were grown by chemical precipitation method using aqueous medium and ambient conditions. All the reaction steps were carried out in a single reaction vessel. All chemicals were of analytical grade and used as received without further purification.

2.1. Synthesis of CdS nanoparticles

100ml Cd $(NO_3)_2$ (0.085M) solution was kept in H_2S atmosphere for 1 minute with vigorous stirring. The stirring was continued for additional 5 hours. The H_2S was supplied through an inlet in a closed reaction vessel while vigorous stirring of the solution to ensure complete mixing and small particle size. The following fundamental reaction was observed for the preparation of CdS nanoparticles $Cd^{2+} + S^{2-} \rightarrow CdS$. Figure 1, shows the reaction setup with Kipp's apparatus attached to the reaction vessel standing on a magnetic stirrer. The solution turned transparent to light yellow as the reaction proceeded. The precipitate thus obtained was washed with water several time prior washing with acetone for 3-4 times and was then air dried.

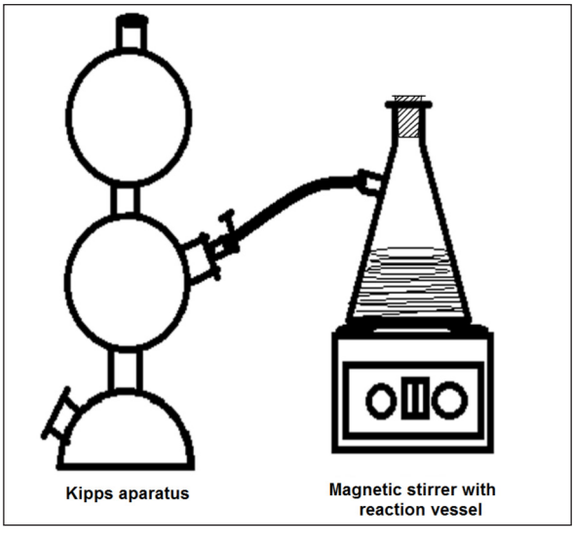

Figure 1: *The reaction setup used in the experiment.*

2.2. Characterization

2.2.1. Optical properties

The UV-Vis spectroscopy has become an effective tool in determining the size and optical properties. The optical properties were determined by using Thermo Spectronics, Genesis 20 Spectrometer in the wavelength range of 400-600 nm at room temperature using the stable dispersions formed in DMSO after ultrasonication. As the particle size decreases, the λ max shifts to shorter wavelengths, due to the band gap increase of the smaller-sized particles [3, 26]. The nature of the electronic transition across the optical band gap is determined by the variation of optical coefficient with wavelength. The nature of the transition is determined using the relation [27]:

$$(\alpha h\nu) = A\,(h\nu - Eg)^{n} \quad [1]$$

Where 'α' is the absorption coefficient, 'A' is a constant related to the effective masses associated with the bands, 'hν' is the energy of photon and n=1/2 for allowed direct transition. The value of absorption coefficient is found to be of the order of 104 cm^{-1} for all composition that supports the direct band gap nature of the semiconductor [28]. The most direct way of extracting the optical band gap is to simply determine the wavelength at which the extrapolations of the base line and the absorption edge cross [27, 29].

With the band gap value, the particle radius can be calculated using equation proposed by Brus [4, 30, 31]. The Brus equation is used to describe the emission energy of quantum dot semiconductor nanocrystals. This expression gives a relation between radius of the crystallite and the energy gap thus explains the quantum size effect.

$$E_g = E_{g0} + \hbar^2\pi^2 / 2R^2\,[1/m_e + 1/m_h] - 1.786\,e^2/\varepsilon R - 0.248\,E_{ry} \quad [2]$$

Where; E_g is the band gap value of the nanoparticles, E_{g0} is the band gap value of the bulk material, m_e and m_h are effective masses of electrons and holes, respectively. ε is the dielectric constant of the semiconductor, R is the radius of the particle, h is the planks constant and E_{ry} is the effective Rydberg energy [4, 32]. The first term in Equation (2) referred to as the quantum localization term (i.e. the kinetic energy term), which shifts the E_g to higher energies proportionally to R^{2-} .The second term in Equation (2) arises due to the screened coulomb interaction between the electron and hole, it shifts the Eg to lower energy as R^{1-}. The third, size-independent term in Equation (2) is the solvation energy loss and is usually small and ignored. In case of semiconductors the effect of the second term, the coulomb interaction term in the equation (2) is very less and hence can be ignored as well. [29, 30]

2.2.2. Thermal properties

Thermal properties were determined by DTA/ TGA/DTG. Thermo Gravimetric Analysis (TGA), Differential Thermogravimetric and Differential Thermal Analysis (DTA) were carried out at a constant rate of 20ºC/min and nitrogen atmosphere. DTA/TGA/DTG measurements were made to reveal the presence of any chemically adsorbed species and to determine thermal stability of the compound. A DTG curve is obtained by plotting the rate of change of weight with time against the temperature. The peak on the derivative curve corresponds to the maximum slope on the TGA curve which indicates the maximum weight loss. The shoulder in the thermogram obtained in DTG, is clearly resolved into peaks. The DTA curve shows the endothermic or exothermic nature of the weight loss leading to thermal decomposition. This event may correspond to the melting point of the compounds.

2.2.3. Structural properties

Structural and morphological properties were determined by Scanning Electron Microscopy (SEM), Transmission Electron Microscopy (TEM), Fourier Transform Infrared Spectroscopy (FTIR) Spectroscopy and X-Ray Diffraction (XRD).

2.2.3.1. Microscopic study (SEM/TEM)

Microscopic studies were done by SEM and TEM. The SEM images were taken, using circular pellets pressed under pressure (4 tones/cm^2) while for TEM

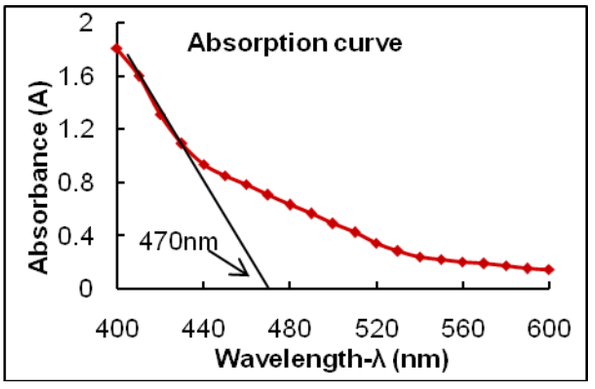

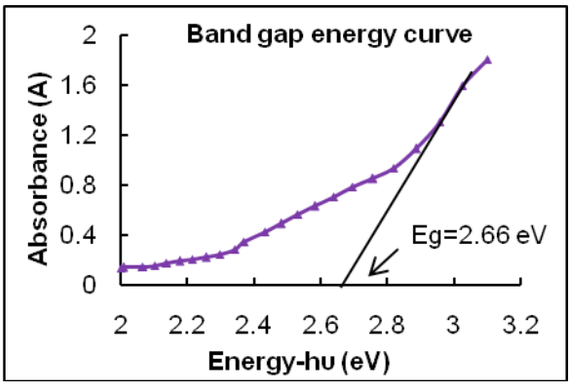

Figure 2: *The absorption curve of the synthesized CdS nanoparticles showing Absorption peak at 470nm*

Figure 3: *The band gap energy (E_g) curve showing the E_g of the synthesized CdS nanoparticles at 2.66eV.*

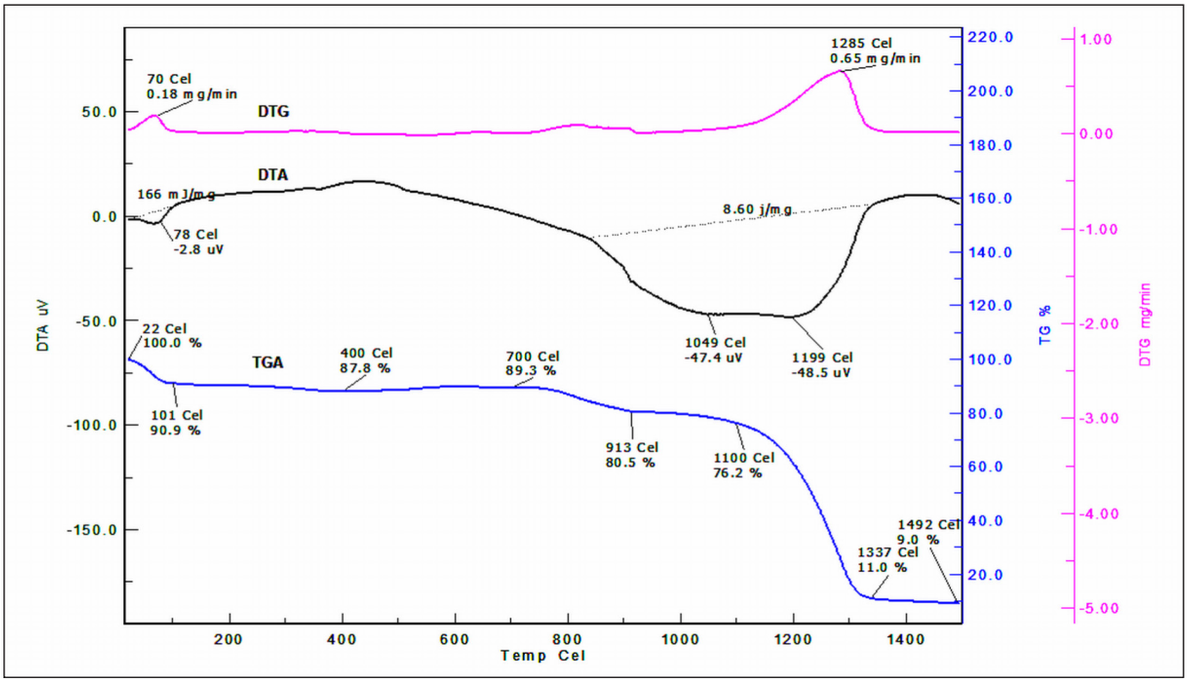

Figure 4: *The DTA/TG/DTG curve of the synthesized nanoparticles.*

the as-prepared CdS nanoparticles were dispersed in acetone by ultrasonication and was placed on carbon coated copper grid.

2.2.3.2. Energy Dispersive X-ray (EDX) spectroscopy

The elemental analysis of the synthesized CdS nanoparticles was done by Scanning Electron Microscopy coupled with Energy Dispersive X-ray (SEM/EDX or EDX) Spectroscopy. SEM, accompanied by X-ray analysis (SEM/EDX), is considered a relatively rapid, inexpensive, and basically non-destructive approach to surface analysis. Purity and composition of the products is studied by EDX. It is often used to survey surface analytical problems, elemental analysis from carbon to uranium and semi-quantitative analysis with detection limits of ~ 0.5 weight % for most elements.

2.2.3.3. Fourier Transform Infrared Spectroscopy (FTIR)

Another method to study the purity and composition of the products is FTIR. The dried CdS nanoparticles mixed with KBr were characterized with FTIR.

2.2.3.4. X-Ray Diffraction Spectroscopy (XRD)

XRD pattern provided information about crystalline phase of the nanoparticles as well as the crystallite size. A considerable broadening of diffraction peaks is the characteristic feature of the x-ray diffraction patterns of films and ultradispersed powders of cadmium sulfide. This broadening of the diffraction peaks is associated with the small sizes of particles in powders or domains in films [34, 35].

Average particle size was found from XRD measurement value of full width at half maxima (FWHM) using Debye-Scherrer formula [36-38].

$$D = K (\lambda / \beta \cos\theta) \quad [3]$$

Where D is the crystallite size, K is a constant (0.91), λ is the wavelength of the CuKα line (1.54Å), θ is the angle between the incident beam and the reflection lattice planes and β is the full width at half maxima (FWHM) of the diffraction peak in radian.

The x-ray diffraction patterns of cadmium sulfide powders closely resemble those of the films. However, the structure of CdS nanopowders, as a rule, has been uniquely determined by researchers either as hexagonal [39, 40] or cubic [41]. In some researches the x-ray diffraction pattern had exhibited pronounced features of both phases, it has been approximated by the sum of the x-ray diffraction patterns of both phases and the results of the analysis have been given as the partial contents of these phases [35]. Some researchers [42] have showed CdS nanocrystals having cubic structure with octahedron and tetragonal morphologies.

3. RESULTS AND DISCUSSIONS

3.1. Optical properties

The absorption edge in bulk CdS was found at 515 nm while in prepared CdS nanoparticles the absorption peak was observed at 470 nm wavelength (Figure 2) which indicates the blue shift in absorption edge. Absorption peak shows shift to shorter wavelength (blue shift) which is in good agreement with the results reported before [29]. Figure (3) shows the plot of Absorbance versus hν whose intercept on energy axis gives the band gap energy Eg of the particles which came out to be 2.66eV (bulk CdS =2.42eV).

The particle radius of the synthesized CdS nanoparticles was calculated from Equation (2) keeping E_{g0}=2.42 eV, m_e=1.73 x 10^{-19}, m_h=7.29 x 10^{-19}, for CdS [4, 12], and E_g=2.66eV (observed) (Figure 3). The particle size came out to be 3.203nm. The prepared CdS nanoparticles had wider band gap than the bulk CdS due to quantum size effect, and can be used in optoelectronics, photonics, photovoltaics, photocatalysis and solar cells.

3.2. Thermal properties

The TGA/DTG curve showed that the compound was thermally stable till 750^{0}C (Figure 4). After 750^{0}C 13.10% weight loss was observed. This can be attributed to the change in phase from octahedron to tetragonal [11]. This is later proved by XRD measurements in this paper. The melting point of the compound was found to be around 1250^{0}C where 96% weight loss was observed. No chemically absorbed species was found as a straight curve was observed till 750^{0}C. However, a very small weight loss (~ 4-5%) was observed before 100^{0}C, which might be due to the presence of moisture or the traces of solvent. The DTA curve showed an endothermic weight loss leading to thermal decomposition. Figure (4) shows the TGA/DTG/DTA curves for the as synthesized CdS nanoparticles. CdS nanoparticles showed good thermal stability and can be used as a pigment in paints and in engineered plastic.

3.3. Structural properties

SEM image (Figure 5) of the surface of the pellet showed smooth structure. TEM image (Figure 6) showed fine spherical CdS particles (quantum dots)

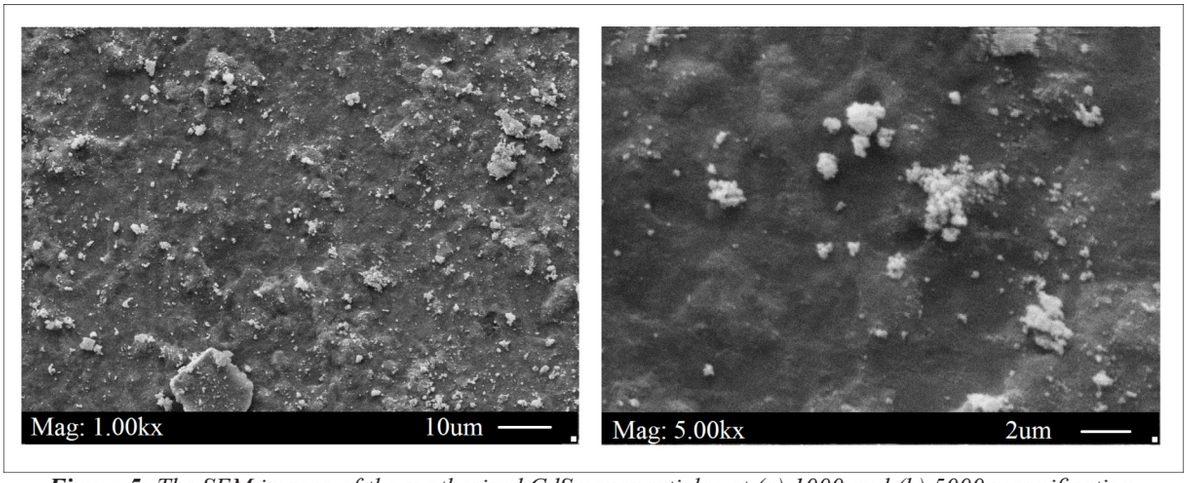

Figure 5: *The SEM images of the synthesized CdS nanoparticles at (a) 1000 and (b) 5000 magnification.*

Table 1: *Interpretation of the peaks obtained by the FTIR Spectra of the synthesized CdS Nanoparticles.*

Peak	Region	Intensity	Interpretation
a	400-470	Small and weak	Cd-S bond stretching (CdS nanoparticles)
b	820-850	Sharp	S-S-S bending or C-H stretching (crystal s-s-s bond or acetone)
c	1060-1120	Sharp	C-O or S-O (acetone or sulphate)
d	1380-1420	Sharp or Broad	C-H bending of CH_3 (Acetone)
e	2340-2360	Small and weak	S-H bond (Free H_2S)
f	3140-3470	Broad	Intermolecular H-bonds (Lattice water)

with some of the particles showing aggregation. The average particle size observed was 4nm. The SEM and TEM images showed the formation of good spherical structure. Thus, the formation of quantum dots was confirmed.

The dried powder samples were analyzed on EDX. The curve in figure (7) reveals the presence of Cd and S peaks confirming the formation of pure Cadmium Sulphide with no other elemental impurity. The average atomic percentage ratio of Cd:S was 54.5:46.5. Other peaks in this figure correspond to carbon, oxygen and silicate which are due to sputter coating of glass substrate on the EDX stage and were not considered in elemental analysis of Cd and S.

The FTIR spectra can be explained by various peaks (Figure 8) obtained by the sample. Table 1 contains the explanation of the peaks obtained by the sample [33].

Figure (9) shows the X-ray diffraction pattern of the as synthesized CdS nanoparticles. In the present work the diffraction patterns of the CdS nanopowder exhibit feature of cubic phase having octahedron and tetragonal morphologies [42]. The data was run on "PowderX" Powder Diffraction Analysis Software (beta version) to get the interpretation done. At room temperature, the XRD pattern of the synthesized CdS nanoparticles shows 3 broad peaks at 25.9, 43.3 and 51.42, the broad peak at 25.9 contains two shoulders at 24.49 (towards left) and at 27.4 (towards right), and a small peak at 29.78 (Figure 9). Interpretation on the basis of Powder-X showed the resulting peak exhibited features of both octahedron and tetragonal phase structures and the results were given as the partial contents of both phases. After heating the sample at 800^{o}C for 1 hour, the octahedron phase disappears and only tetragonal structural phase was observed with three sharp peaks at 24.5, 29.22 and 35.08 (Figure 10).

This also explains the 13.10% weight loss after 750^{0}C in TGA, as the tetragonal phase is more

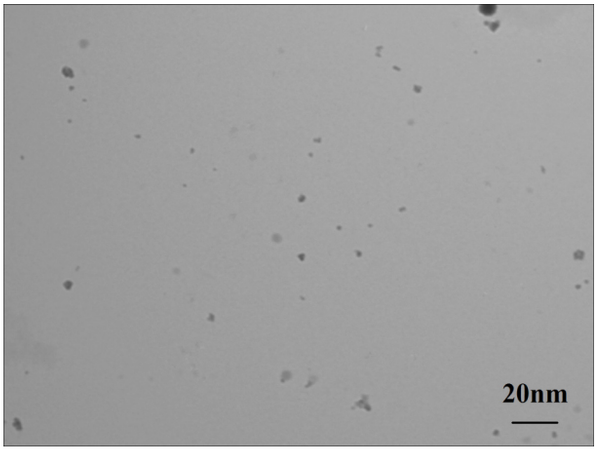

Figure 6: *TEM image of the synthesized CdS nanoparticles showing spherical quantum dots with some particles showing aggregation.*

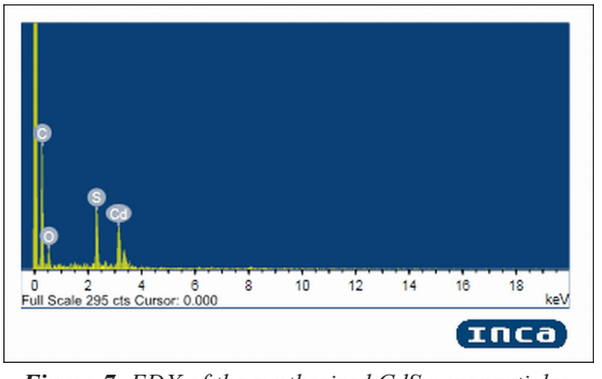

Figure 7: *EDX of the synthesized CdS nanoparticles.*

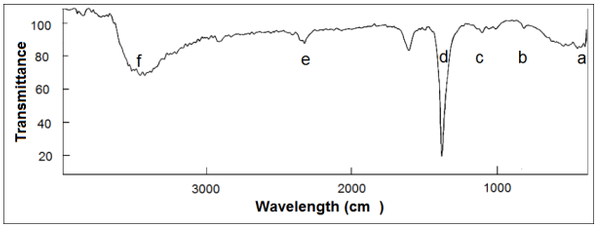

Figure 8: *The figure showing FTIR pattern of the synthesized CdS nanoparticles.*

stable than octahedron phase. It is assumed that the particles with octahedron phase structure either disintegrated or undergone phase change. A similar observation was done by C.C. Chen and group [11]. The average crystallite size calculated by the Debye- Scherrer formula using FWHM values of the prominent peaks came out to be 8.15nm.

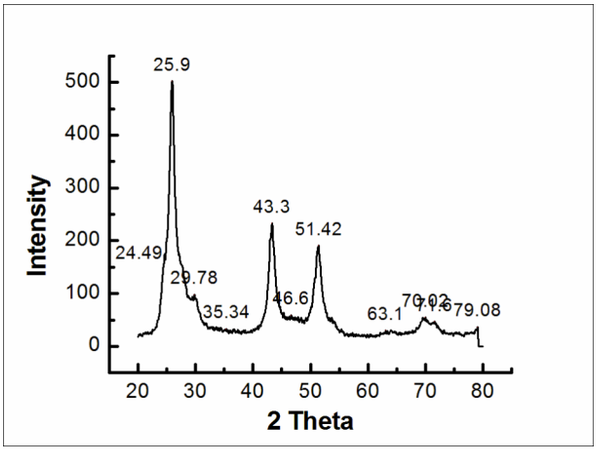

Figure 9: *The XRD pattern of the as synthesized CdS nanoparticles showing both octahedron and tetragonal morphologies.*

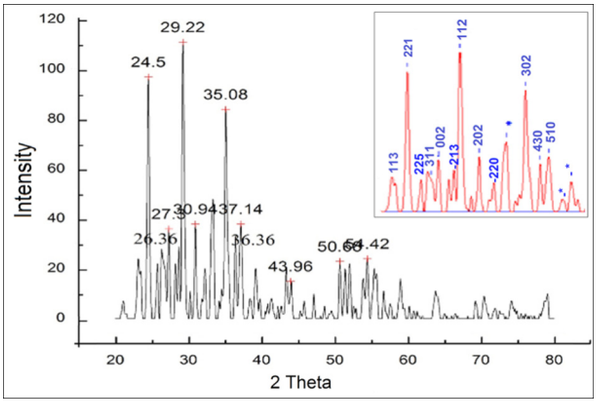

Figure 10: *The XRD pattern of CdS nanoparticles after heating them at 800^{0}C for 1 hour. The inset shows the XRD peaks exhibiting features of tetragonal crystal phase.*

4. CONCLUSIONS

II –VI semiconductor CdS nanocrystals were synthesized via single pot chemical precipitation method at ambient conditions. The Optical Absorption peak was observed at 470 nm wavelength while that of bulk is 515nm indicating the blue shift in absorption edge also the band gap calculated from absorption spectra was at 2.66eV while the bulk CdS has 2.42eV showing quantum size effect.

The formation of good spherical structure proved the formation of quantum dots. The Thermal spectra showed thermally stable nanoparticles, the melting point of the CdS nanoparticle was 1250^0C where 96% weight loss was observed, the nanoparticles were thermally stable upto temperature as high as 750^0C, and only a small weight loss (13.10%) was observed in between 750^0-800^0C. The XRD pattern of the CdS nanoparticles showed both octahedron and tetragonal crystal structure which after heating at 800^0C for 1 hour, showed only tetragonal structural phase.

This can be attributed to the weight loss at 750^0C in TGA. The particle size calculated from Absorption spectra, Diffraction spectra and Microscopic studies was found to be in the range 3-8nm and showed good agreement with each other. Thus, the synthesized nanoparticles showed quantum size effect and good thermal stability with crystalline nature. The quantum dots prepared have great practical utility and can be exploited in field of electronic, optics, photocatalysis, solar cells, optoelectronics, photonics, and photovoltaics.

ACKNOWLEDGMENTS

The authors are thankful to Uttar Pradesh Council of Science and Technology (UPCST), Lucknow for funding the project (CST/SERPD/D-1888), Centre of Excellence in Materials Science (Nanomaterials), Department of Applied Physics, Z.H.C.E.T., A.M.U., Aligarh, for providing the facility of XRD and Shoeb Khan for providing the facility of TEM and TGA/DTG/TGA.

REFERENCES

1. Halperin, W. P., "Quantum size effects in metal particles," Rev. Mod. Phys., Vol. 58, No. 3, (1986), pp. 533-607.
2. Lippens, P. E. and Lannoo, M., "Calculation of the band gap for small CdS and ZnS crystallites," Phys. Rev. B, Vol. 39, No. 15, (1989), pp. 10935-10942.
3. Khairutdinov, R. F., "Chemistry of semiconductor nanoparticles," Russ. Chem. Rev., Vol. 67, No. 2, (1998), pp. 109-122.
4. Wang, Y. and Herron, N., "Quantum size effects on the exciton energy of CdS clusters," Phys. Rev. B, Vol. 42, No. 11, (1990), pp. 7253-7255.
5. Narayanan, S. S. and Pal, S. K., "Aggregated CdS Quantum Dots: Host of Biomolecular Ligands," J. Phys. Chem. B, Vol. 110, (2006), pp. 24403-24409.
6. Mthethwa, T., Pullabhotla, V. S. R. R., Mdluli, P. S., Smith, J. W. and Revaprasadu, N., "Synthesis of hexadecylamine capped CdS nanoparticles using heterocyclic cadmium dithiocarbamates as single source precursors," Polyhedron, Vol. 28, (2009), pp. 2977-2982.
7. Li, C., Liu, Z. and Yang, Y., "The selective synthesis of single-crystalline CdS nanobelts and nanowires by thermal evaporation at lower temperature", Nanotechnology, Vol. 17, (2006), pp. 1851-1857.
8. Goldstein, A. N., Echerand, C. M. and Alivisatos, A. P., "Melting in semiconductor nanocrystals," Science, Vol. 256, (1992), pp. 1425-1427.
9. Rajeshwar, K., Tacconi, N. R. and Chenthamarakshan, C. R., "Semiconductor-based composite materials: preparation, properties, and performance," Chem. Mater., Vol. 13, (2001), pp. 2765-2782.
10. Banerjee, R., Jayakrishnan, R. and Ayyub, P., "Effect of the size-induced structural transformation on the band gap in CdS nanoparticles," J. Phys. Condens. Matter, Vol. 12, No. 50, (2000), pp. 10647-10650.
11. Chen, C. C., Herhold, A. B., Johnson, C. S. and Alivisatos, A. P., "Size Dependence of Structural Metastability in Semiconductor Nanocrystals," Science, Vol. 276, (1997), pp. 398-401.
12. Singh, V. and Chauhan, P., "Synthesis and structural properties of wurtzite type CdS nanoparticles, Chalcogenide Lett.,Vol. 6, No. 8, (2009), pp. 421-426.
13. Acevedo, A. M., "Can we improve the record efficiency of CdS/CdTe solar cells?," Sol. Energy Mater. & Sol. Cells, Vol. 90, No. 15, (2006), pp. 2213-2220.
14. Lin, C. F., Lianga, E. Z., Shjh, S. M. and Si, W. F., "CdS-nanoparticle light-emitting diode on Si,"

Proc. SPIE., Vol. 4641, (2002), pp. 102-110.

15. Murai, H., Abe, T., Matsuda, J., Sato, H., Chiba, S. and Kashiwaba, Y., "Improvement in the light emission characteristics of CdS:Cu/CdS diodes," Appl. Surf. Sci., Vol. 244, (2005), pp. 351-354.
16. Duan, X., Huang, Y., Agarwal, R. and Lieber, C. M., "Single-nanowire electrically driven lasers," Nature, Vol. 421, (2003), pp. 241-245.
17. Zhong, Z., Qian, F., Wang, D. and Lieber, C. M., "Synthesis of p–Type Gallium nitride nanowires for electronic and photonic nanodevices," Nano Lett., Vol. 3, No. 3, (2003), pp. 343-346.
18. Dai, G., Zou, B. and Wang, Z., "Preparation and periodic emission of superlattice CdS/CdS: SnS_2 Microwires," J. Am. Chem. Soc., Vol. 132, (2010), pp. 12174–12175.
19. Sejdic, J. T., Peng, H., Cooney, R. P., Bowmaker, G. A., Cannell, M. B. and Soeller, C., "Amplification of a conducting polymer-based DNA sensor signal by CdS nanoparticles," Curr. Appl. Phys., Vol. 6, (2006), pp. 562–566.
20. Li, X., Jia, Y., Wei, J., Zhu, H., Wang, K., Wu, D. and Cao, A., "solar cells and light sensors based on nanoparticle-grafted carbon nanotube films," Acs Nano, Vol. 4, No. 4, (2010), pp. 2142–2148.
21. Wang, Y., Ramanathan, S., Fan, Q., Yun, F., Morkoe, H. and Bandyopadhyay, S., "Electric field modulation of infrared absorption at room temperature in electrochemically self assembled quantum dots," J. Nanosci. Nanotechnol., Vol. 6, No. 7, (2006), pp. 2077-2080.
22. Romeoa, N., Bosioa, A., Mazzamutoa, S., Romeob, A. and Vaillant-Rocac, L., "High efficiency cdte/cds thin film solar cells with a novel back-contact," In Proceedings of 22nd European Photovoltaic Solar Energy Conference, Milan, Italy, 3-7 September, (2007), pp. 1919-1921.
23. Zyoud, A. H., Zaatar, N., Saadeddin, I., Ali, C., Park, D., Campet, G. and Hilal, H. S., "CdS-sensitized TiO_2 in phenazopyridine photo-degradation: Catalyst efficiency, stability and feasibility assessment," J. Hazard. Mater., Vol. 173, (2010), pp. 318–325.
24. Zhu, H., Jiang, R., Xiao, L., Chang, Y., Guan, Y., Li, X. and Zeng, G., "Photocatalytic decolorization and degradation of Congo Red on innovative crosslinked chitosan/nano-CdS composite catalyst under visible light irradiation," J. Hazard. Mater., Vol. 169, (2009), pp. 933–940.
25. Acharya, K. P., Photocurrent Spectroscopy of CdS/plastic, CdS/glass, and ZnTe/GaAs hetero-pairs formed with pulsed-laser deposition, Ph.D. Dissertation, Graduate College of Bowling Green State University, (2009).
26. Yang, Y. J., He, L. Y. and Xiang, H., "Electrochemical synthesis of free-standing CdS nanoparticles in ethylene glycol," Russ. J. Electrochem., Vol. 42, No. 9, (2006), pp. 954-958.
27. Mathew, X., Sebastian, P. J., Sanchez, A. and Campos, J., "Structural and opto-electronic properties of electrodeposited CdTe on stainless steel foil - photovoltaic energy conversion," Sol. Energy Mater. & Sol. Cells, Vol. 59, No. 16, (1999), pp. 99-114.
28. Barote, M. A., Yadav, A. A., Deshmukh, L. P. and Masumdar, E. U., "Synthesis And Characterization of Chemically Deposited $Cd_{1-X}Pb_xS$ Thin Films," J. Non-Oxide Glasses, Vol. 2, No. 3, (2010), pp. 151-165.
29. Martinez-Castanon, G. A., Sanchez-Loredo, M. G., Martinez-Mendoza, J. R. and Ruiz, F., "Synthesis of CdS nanoparticles: a simple method in aqueous media," AZojomo, Vol. 1, (2005), pp. 1-7.
30. Brus, L., "Electronic wave functions in semiconductor clusters: experiment and theory," J. Phys. Chem., Vol. 90, (1986), pp. 2555-2560
31. Brus Equation [Online]. From Wikipedia, the free encyclopedia. http://en.wikipedia.org/w/index.php?oldid=433920424 (accessed on July 2, 2011)
32. Baset, S., Akbarib, H., Zeynali, H. and Shafie, M., "Size measurement of metal and semiconductor nanoparticles via UV-Vis absorption spectra," Dig. J. Nanomater. Bios., Vol. 6, No. 2, (2011), pp. 709–716.
33. Socrates, G., "Infrared Characteristic Group Frequenciesa", John Wiley & Sons, New York, (1980).
34. Rempel, A. A., Kozhevnikova1, N. S., Berghe, S. V., Renterghem, W. V. and Leenaers, A. J. G., "Self-organization of cadmium sulfide nanoparticles on the macroscopic scale," Phys. Stat. Sol. (B), Vol. 242, No. 7, (2005), pp. 61–63.
35. Vorokh, A. S. and Rempel, A. A., "Atomic structure

of cadmium sulfide nanoparticles," Phys. Solid State, Vol. 49, No. 1, (2007), pp. 148–153.

36. Patterson, A. L., "The Scherrer formula for X-ray particle size determination," Phys. Rev. Lett., Vol. 56, (1939), pp. 978-982.
37. Als-Nielsen, J. and McMorrow, D., "Elements of Modern X-Ray Physics," Wiley, (2001).
38. S. Mukherjee, S. Kumar, and D. Das, "Tailoring Magnetic Responses of Nanoscale Integrated Magnetite and Cadmium Sulphide: Microstructural, Magnetic and Hyperfine Studies", Nanosci. Nanotechnol. Lett., Vol. 4, (2012), pp.110–116.
39. Zhang, J., Sun, L., Liao, C. and Yan, C., "Size control and photoluminescence enhancement of CdS nanoparticles prepared via reverse micelle method," Solid State Commun., Vol. 124, (2002), pp. 45–48.
40. Ximello-Quiebras, J. N., Contreras-Puente, G., Aguilar-Hernandez, J., Santana-Rodriguez, G. and Arias-Carbajal Readigos, "A Physical properties of chemical bath deposited CdS thin films," Sol. Energy Mater. & Sol. Cells, Vol. 82, (2004), pp. 263–268.
41. Pathania, D., Sarita and Rathore, B. S., "Synthesis, Characterization and photocatalytic application of bovine serum albumin capped cadmium sulphide nanoparticles," Chalcogenide Lett., Vol. 8, No. 6, (2011), pp. 396–404.
42. Ricolleau, C., Audinet, L., Gandais, M., Gacoin, T. and Boilot, J. P., "3D morphology of II-VI semiconductor nanocrystals grown in inverted micelles," J. Cryst. Growth, Vol. 203, (1999), pp. 486-499.

Highlights for review:

- Novel synthetic procedure.
- Optical properties, Quantum size effect and Quantum Dots.
- Thermal and Structural properties.
- Determination of Crystal structure and particle size by XRD.
- Determination of practical utility of the compound.